J Mater Sci (2009) 44:6135–6143
DOI 10.1007/s10853-009-3848-2

Phase transformation and precipitation behavior of niobium component out of niobium-doped anatase-type TiO_2 nanoparticles synthesized via hydrothermal crystallization

Masanori Hirano · Yoshiko Ichihashi

Received: 17 February 2009 / Accepted: 25 August 2009 / Published online: 10 September 2009

Abstract The precipitation behavior of niobium component out of niobium-doped anatase-type TiO_2 and structural change in the course of heating were investigated. The samples were directly formed under hydrothermal conditions at 240 °C for 5 h in the presence of aqueous ammonia via crystallization from co-precipitates that were obtained from precursor solutions of $TiOSO_4$ and $NbCl_5$. The as-prepared niobium-doped anatase-type titania nanoparticles showed bluish color and absorption in the visible region, which was confirmed to be due to the presence of Ti(III) in the solid solutions using electron paramagnetic resonance measurement. The niobium-doped anatase-type titania existed stably without an appearance of any other phases after heating up to 500 °C for 1 h. In the course of heating at 500–800 °C, continual and clear decrease in the lattice parameters a_0 and c_0 of the anatase was observed, which was followed by the precipitation of Nb_2O_5 and $TiNb_2O_7$ out of the niobium-doped anatase, but the anatase phase was maintained without anatase-to-rutile phase transformation up to 850–1,000 °C. The anatase-to-rutile phase transformation was gradually retarded when the niobium content increased.

Introduction

Titanium dioxide (titania, TiO_2) is well known to be synthesized in three distinct polymorphic forms, anatase, rutile, and brookite, despite rutile being the most stable phase at any temperature. Recently, extensive attention has been focused on titania as photocatalysis [1] and for solar energy conversion in wet-type solar cells [2], among various kinds of semiconductor oxides commonly used. It is well known that the metastable anatase-type titania shows higher photoactivity than other phases. On the other hand, titania as well as zirconia has been useful as gas sensing materials, mainly in oxygen sensor (lambda sensor) devices because of its dual response to both oxygen-rich and oxygen-lean atmosphere and its stability at temperature up to 700 °C [3].

The crystallization of titania into different structures depends on its preparation technique or crystallization method and their conditions, e.g., precursor materials and their concentration, composition, pH, treatment temperature, the rate of crystallization, and so on since the difference in phase stability between stable rutile and metastable anatase and brookite is slight at low temperatures. The phase stability and phase transformation behavior of anatase-type and brookite-type titania also strongly depends on cation impurities [4–15] and anion impurities [14] present in the system, grain (crystallite) size [15], and preparation conditions such as reaction atmosphere. In order to apply titania at high temperatures as gas sensors and catalysts, a phase stable anatase becomes necessary [16]. The control of anatase-to-rutile phase transformation is one of the important problems for high temperature applications of sensors and catalysts [17]. We have reported that the phase stability of anatase can improve up to 1,300 °C via direct formation of anatase (TiO_2)/silica composite nanoparticles under hydrothermal conditions [18].

To form homogeneous anatase-type TiO_2 nanocrystals with dopant through solid-state reaction with heat treatment at 600–1,000 °C is not so easy because pure anatase phase easily changes to stable rutile one by heat treatment above 635 °C from the result of the kinetic study [19, 20]. Hydrothermal treatment can synthesize nanocrystalline

M. Hirano (✉) · Y. Ichihashi
Department of Applied Chemistry, Faculty of Engineering,
Aichi Institute of Technology, Yakusa, Toyota 470-0392, Japan
e-mail: hirano@aitech.ac.jp

solid solutions and metastable compounds at relatively low temperatures [21]. Through hydrothermal technique, nanometer-sized particles of anatase-type titania doped with different cations have been prepared [11, 12, 22–24].

Niobium(V) oxide (Nb_2O_5) has been known to be useful as promoters and supports of catalysts and as unique solid acid catalysts [25]. Titania photocatalysts doped with 0.02–1.0 at.% Nb^{5+} were reported to be prepared via sol–gel method from titanium isopropoxide and niobium ethoxide and crystallization by calcination at 450 °C [26]. The importance and influence of niobium doping into titania for oxygen sensors have also been emphasized in order to improve device sensitivity at lower working temperature [27, 28]. The formation of niobium-doped titania nanocrystals by hydrothermal method using the hydrolysis of urea and their good photocatalytic activity have been reported [22, 29]. However, there is a lack of information on the valence state of titanium and niobium in those metastable anatase-type titania nanocrystals doped with niobium and their thermal change in structure and phase stability. Although many articles discuss on the influence of niobium doping into anatase, there exist uncertainty on phase stability and phase transformation behavior of niobium-doped anatase. In our previous work, new anatase-type solid-solutions of $Al_XTi_{1-2X}Nb_XO_2$ [30] and $Sc_XTi_{1-2X}Nb_XO_2$ [31] in the range $X = 0$–0.20 that were co-doped with equivalent atomic fraction of niobium(V) and either aluminum(III) or scandium(III) to titanium(IV) were directly synthesized as nanocrystalline particles using the mild hydrothermal synthesis. In these studies, anatase-type titania doped with niobium + aluminum or niobium + scandium transformed into their single phase of stable rutile without a trace of precipitations out of titania phase through heat treatment.

The present study was concerned with investigation on the structural change and phase stability of relatively large amount of niobium-doped anatase-type titania nanocrystals, especially observation on the segregation and precipitation behavior of niobium component out of niobium-doped anatase, accompanied with change (decrease) in lattice parameters of anatase in the course of heating. The samples were directly synthesized at 240 °C via hydrothermal crystallization of co-precipitates in the presence of aqueous ammonia. The valence state of titanium and niobium in the as-prepared titania nanoparticles doped with niobium was also confirmed using electron paramagnetic resonance (EPR) measurements.

Experimental procedure

A mixture of an aqueous solution of reagent-grade $TiOSO_4$ and ethanol solution of $NbCl_5$ in different ratios of Ti/Nb with total cation concentrations (Ti + Nb) of 0.1 mol/dm^3 was prepared in a Teflon container. The solution mixture containing co-precipitates was prepared and controlled to be weak basic condition by the addition of aqueous solution of ammonia with stirring. This solution mixture in the Teflon container was then placed in a stainless-steel vessel. After the vessel was tightly sealed, it was heated at 200–240 °C for 5 h under rotation at 1.5 rpm. After hydrothermal treatment, the precipitates were washed with distilled water until the pH value of the rinsed water became 7.0, separated from the solution by centrifugation, and dried in an oven at 60 °C. The powders thus prepared were heated in an alumina crucible at heating rate 200 °C/h, held at 500–1150 °C for 1 h in air, and then cooled to room temperature in a furnace.

The as-prepared and heated powders were examined using X-ray diffractometry (XRD; model RINT-2000, Rigaku, Tokyo, Japan) with Cu Kα radiation and observed under transmission electron microscopy (TEM; model JEM-2010, JEOL, Tokyo, Japan). The crystallite size of anatase was estimated from the line broadening of 101 diffraction peak, according to the Scherrer equation: $D_{XRD} = K\lambda/\beta\cos\theta$, where θ is the Bragg angle of diffraction lines; K a shape factor ($K = 0.9$ in this work); λ the wavelength of incident X-rays, and β the corrected half-width given by: $\beta^2 = \beta_m^2 - \beta_s^2$, where β_m is the measured half-width and β_s the half-width of a standard sample. The lattice parameters were measured using silicon as the internal standard. The amounts of rutile phase formed in the heated samples were calculated from the equation [32]:

$$F_R = 1/\{1 + 0.79[I_A(101)/I_R(110)]\},$$

where F_R is the mass fraction of rutile in the samples, and $I_A(101)$ and $I_R(110)$ the integrated 101 intensities of anatase and 110 of rutile, respectively, these lines were at $\sim 26°$ in 2θ. The chemical composition of the resultant powders was analyzed using an inductively coupled plasma emission spectrometer (ICP; model ICP575II, Nippon Jarrell-Ash, Japan). The optical absorption of these prepared powders was measured using an ultraviolet–visible spectrophotometer (V-560, Nihon Bunko, Tokyo, Japan). The EPR (or electron spin resonance (ESR)) spectra were recorded at 10 K on a spectrometer (ESP 350E, BRUKER) operating in the X band mode at 9.46 GHz, having a TM 110 cavity.

Results and discussion

Preparation and characterization of niobium-doped anatase-type titania samples

The XRD patterns of precipitates obtained under hydrothermal conditions at 240 °C are shown in Fig. 1. The

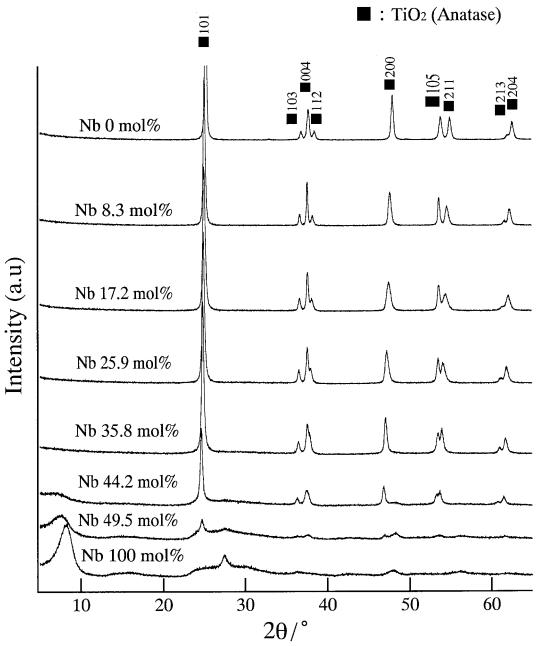

Fig. 1 X-ray diffraction patterns of precipitates obtained from solution mixtures of $TiOSO_4$ and $NbCl_5$ in the presence of aqueous ammonia with total metal cation concentration of 0.1 mol/dm^3 under hydrothermal conditions at 240 °C for 5 h

Table 1 Analytical value of Nb, crystallite size, and optical band gap of as-prepared niobium-doped anatase-type titania samples formed under hydrothermal conditions at 240 °C for 5 h

Sample	Analytical value of Nb (mol.%)	Crystallite size (nm)	Optical band gap E_d (eV)
a	0	30	3.25
b	8.3	28	3.18
c	17.2	26	3.18
d	25.9	34	3.18
e	35.8	29	3.19
f	44.2	–	–
g	49.5	–	–
h	100		

compositions of the precipitates shown in the XRD patterns are analytical value of niobium (Nb/(Ti + Nb) mol.%) in the as-prepared samples determined using ICP, which are listed in Table 1. Anatase-type titania was only detected as crystalline phase in the as-prepared solid precipitates containing niobium up to 35.8 mol.%, and no trace of diffraction peaks due to another crystalline phase were detected. However, the probable presence of amorphous phase in the precipitates is suggested in the sample Nb 44.2 mol.% because of a slight change in background of XRD patterns.

Figure 2 shows detail of the region around $2\theta = 54°$ in the XRD patterns of the samples shown in Fig. 1. It

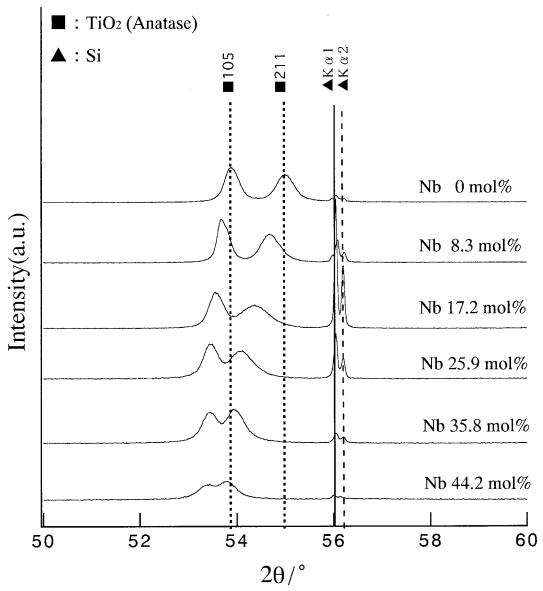

Fig. 2 Detail of the region around 54° 2θ of the XRD patterns of precipitates with various contents of niobium

indicates the compositional dependence of the shift of the 105 and 211 lines in the XRD patterns of niobium-containing anatase-type titania samples. The 105 and 211 diffraction lines (in Fig. 2) and the 101 lines (in Fig. 1) of anatase are clearly observed to shift gradually toward lower diffraction angles 2θ when the niobium content is increased in the precipitates, which is consistent with the formation of anatase solid solutions with niobium oxide. A gradual increase in the lattice parameters a_0 and c_0 of anatase was observed when the niobium content was increased. It is interesting that titania doped with relatively large amount of niobium is formed as metastable anatase phase through hydrothermal crystallization.

The TEM images of the as-prepared 8.3 and 17.2 mol.% niobium-doped anatase precipitates are shown in Fig. 3a, b, respectively. The morphology of the particles is not so uniform and the particle sizes of the precipitates estimated from the TEM images were around 20–35 nm. The crystallite sizes of anatase in the as-prepared samples containing 0–35.8 mol.% niobium estimated from the line broadening of the 101 anatase peak in the XRD patterns are listed in Table 1. The crystallite sizes of anatase were around 28–34 nm.

The effect of the treatment temperature on the crystallization of niobium-doped anatase-type titania from the co-precipitates under hydrothermal conditions was investigated. The XRD patterns of the precipitates obtained at the starting composition of 35 mol.% niobium under hydrothermal conditions at various temperatures for 5 h are shown in Fig. 4. The precipitation of crystalline phase, i.e., the crystallization of anatase from the amorphous phase of co-precipitates begins to appear at hydrothermal treatment

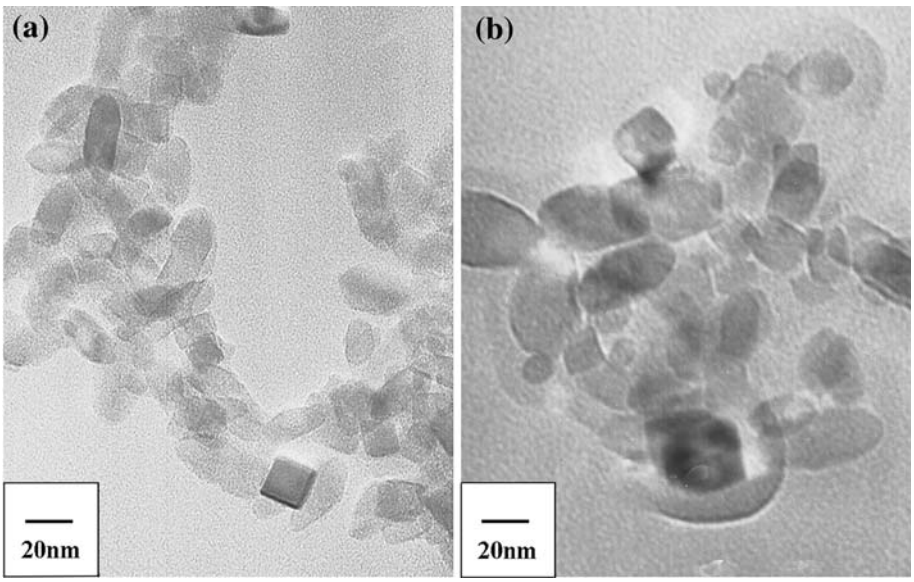

Fig. 3 Transmission electron microscopy images of precipitates containing **a** 8.3 and **b** 17.2 mol.% niobium

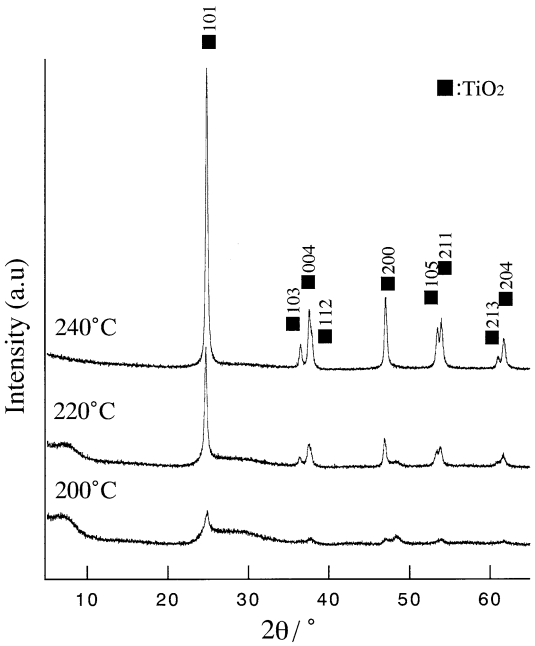

Fig. 4 X-ray diffraction patterns of precipitates obtained from solution mixtures of $TiOSO_4$ and $NbCl_5$ at the composition of 35 mol.% niobium in the presence of aqueous ammonia with total metal cation concentration of 0.1 mol/dm^3 under hydrothermal conditions at various temperatures for 5 h

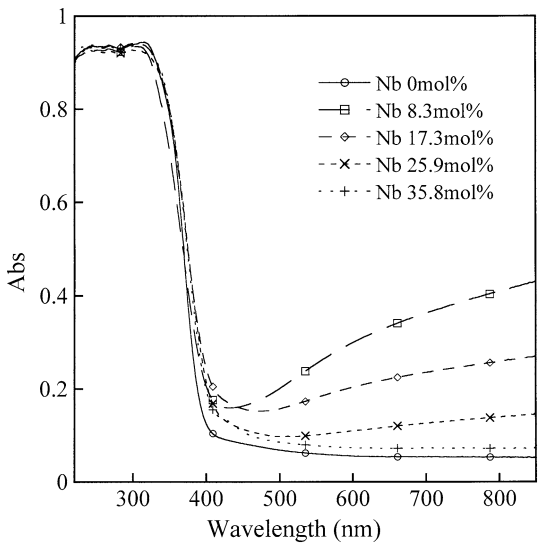

Fig. 5 Diffuse reflectance spectra of as-prepared anatase-type precipitates with various contents of niobium

temperature around 200 °C. At this composition containing relatively large amount of niobium, hydrothermal treatment more than 240 °C is considered to be necessary for the formation of anatase with sufficient crystallinity.

The diffuse reflectance spectra of the as-prepared niobium-doped titania having anatase-type structure, are shown in Fig. 5. The optical band gap is obtained from the diffuse reflectance spectra of the samples, using $\alpha h\nu = \text{const}\ (h\nu - E_g)^n$, where α is the absorption coefficient, $n = 1/2$ for a direct allowed transition. The band-gap values for the anatase-type titania doped with niobium are listed in Table 1, which were determined from the energy intercept by extrapolating the straight regions of the plot of $(\alpha h\nu)^2$ versus the photon energy $h\nu$ for a direct allowed transition (E_d). Slight decrease in band-gap value of anatase was observed when small amount of niobium was doped into anatase. The band-gap value did not show noticeable change over the compositional range 8.3–35.8 mol.% niobium. The as-prepared anatase-type titania doped with 8.4–25.9 mol.% niobium showed bluish color and absorption in the visible region, as shown in Fig. 5.

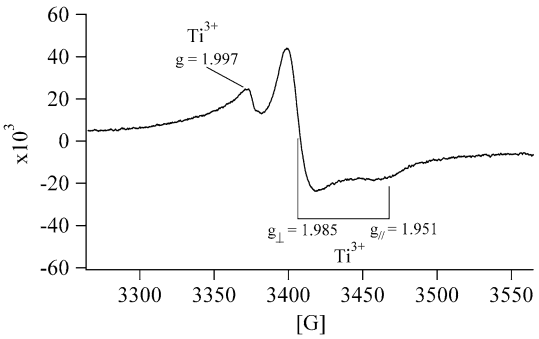

Fig. 6 Electron paramagnetic resonance spectrum of as-prepared anatase-type titania doped with 8.3 mol.% niobium

The valence states of titanium and niobium in the samples have been investigated using EPR measurements. Figure 6 shows the EPR spectrum of as-prepared titania doped with 8.3 mol.% niobium. This sample shows the most bluish color and large absorption in the visible region (Fig. 5). The EPR spectrum of titania containing 8.3 mol.% niobium exhibits three signals of $g = 1.997$, 1.985, and 1.951, which corresponds to Ti^{3+}. The EPR measurements showed that the presence of titanium with valence of three in the niobium-doped titania samples. No signal corresponding to Nb^{4+} was confirmed in the spectrum. This showed that niobium existed as valence of five in the sample.

Precipitation of niobium component out of anatase during heating

The phase stability of metastable anatase during heating in air was investigated. Figure 7 shows XRD patterns of the samples containing 0–35.8 mol.% niobium after heating at 800 °C for 1 h. An appearance of $TiNb_2O_7$ phase and the coexistence of a slight amount of Nb_2O_5 phase with the anatase phase in some cases are observed in the XRD patterns. The increase in the intensity of $TiNb_2O_7$ phase is observed when the niobium content in the samples is increased. It is important to investigate whether this niobium component of $TiNb_2O_7$ and Nb_2O_5 phases came out of the niobium-doped anatase or whether they were formed by the crystallization of amorphous phase contained in the as-prepared precipitates.

In Fig. 8a, the XRD patterns of the sample containing 35.8 mol.% niobium before and after heating at 500–950 °C for 1 h are shown. Figure 8b shows the details of the region around $2\theta = 15$–30° in the XRD patterns of the samples. In the samples before and after heating at 500 °C, only a single phase of anatase existed as crystalline phase. The change in crystalline phase of the samples after heating at less than 500 °C was not observed. After heating the sample at 650 °C, an appearance of small amount of Nb_2O_5

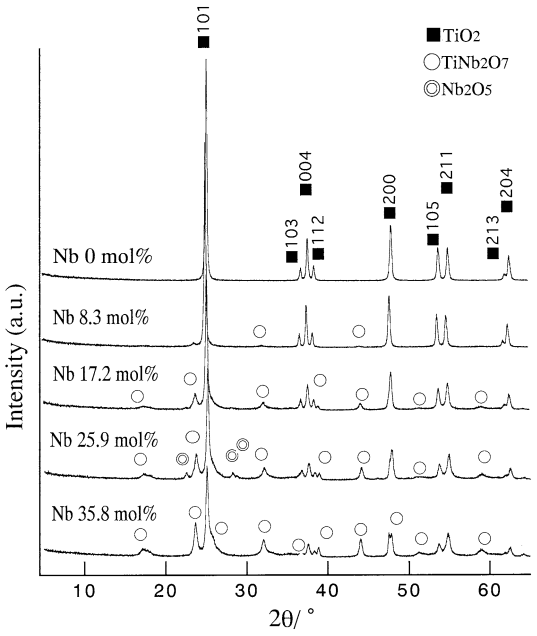

Fig. 7 X-ray diffraction patterns of 0–35.8 mol.% niobium containing TiO_2 heated at 800 °C for 1 h in air

phase accompanied with the shift of the 101 diffraction line of anatase to a higher diffraction angles was detected in the XRD pattern (Fig. 8b). When the heating temperature is increased from 500 to 750 °C, the gradual shift of the 101 diffraction line of anatase to a higher diffraction angles is clearly observed in the sample, which is accompanied with the precipitation of the Nb_2O_5 phase out of the anatase phase as shown in Fig. 8b. A $TiNb_2O_7$ phase appears coexisting with the Nb_2O_5 phase in the samples after heating at 700–750 °C. It is supposed that the Nb_2O_5 and $TiNb_2O_7$ phase came out of the anatase because of the followed gradual shift of the 101 diffraction line of anatase as shown in Fig. 8b. The Nb_2O_5 phase disappears in the samples heated at 800 °C. The crystalline phases present in the samples heated at 800–950 °C are anatase-type titania and $TiNb_2O_7$ phase, and no trace of diffraction peaks due to rutile phase are detected.

Figure 9 shows change in the lattice parameters a_0 and c_0 of anatase in the samples containing 35.8 mol.% niobium with heating temperature. It is interesting that gradual, continual, and clear decrease in the lattice parameters a_0 and c_0 of the anatase was observed in the course of heating at 500–800 °C with increasing heating temperature, which is followed by the precipitation of Nb_2O_5 phase and $TiNb_2O_7$ phase out of the metastable anatase-type titania doped with niobium that was directly formed by hydrothermal method. The change in the lattice parameters a_0 and c_0 was not observed between the samples heated at 800 and 950 °C, which value is a bit larger than those of pure anatase-type TiO_2 free from niobium and the JCPDS

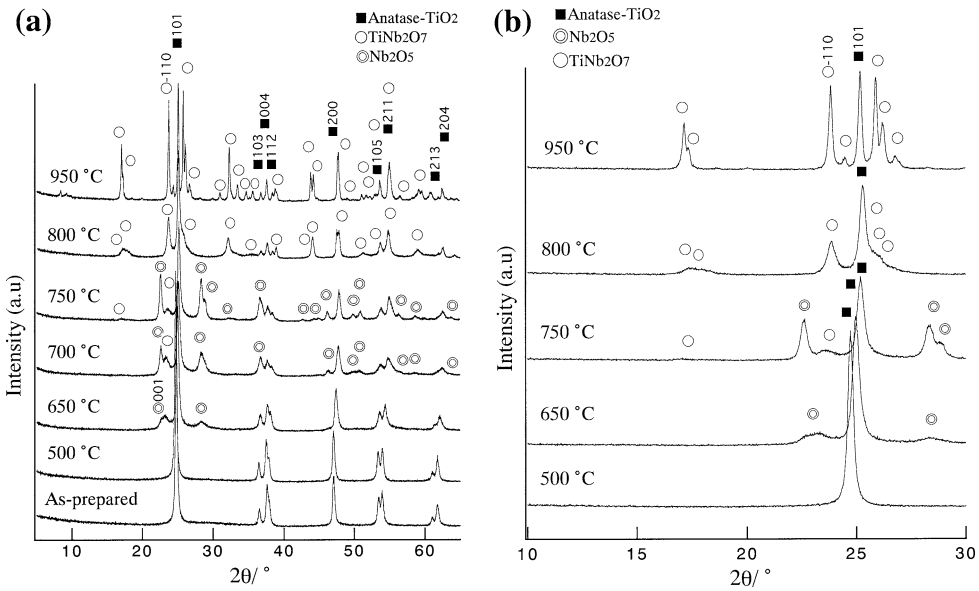

Fig. 8 **a** X-ray diffraction patterns of 35.8 mol% niobium containing TiO_2 before and after heated at 500–950 °C for 1 h in air. **b** Detail of the region around 25° 2θ of the X-ray diffraction patterns of 35.8 mol.% niobium containing titania after heated at 500–950 °C for 1 h in air

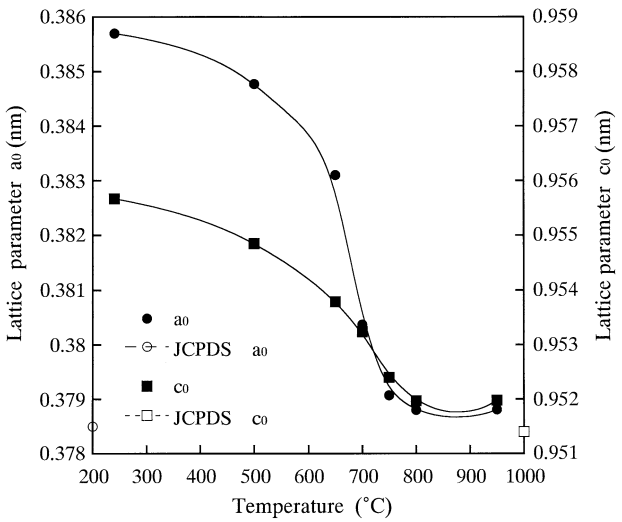

Fig. 9 Lattice parameters a_0 and c_0 of anatase in the sample containing 35.8 mol.% niobium versus heating temperature

data. This result supports that the appearance of Nb_2O_5 and $TiNb_2O_7$ phase is not because of the crystallization from the amorphous phase contained in the samples, but results from the precipitations out of the anatase. The amount of niobium soluble into anatase-type titania phase in the course of heating at 800–950 °C was considerably limited, since most of niobium component separated from the anatase phase was precipitated as $TiNb_2O_7$ phase before anatase-to-rutile phase transformation. On the other hand, it is worth noting that anatase-type $Al_XTi_{1-2X}Nb_XO_2$ [30] or $Sc_XTi_{1-2X}Nb_XO_2$ [31] solid solutions co-doped with equivalent atomic fraction of niobium(V) and aluminum(III) or niobium(V) and scandium(III) to titanium(IV) transformed into their single phase of stable rutile and did not separate the added components as precipitation phase out of the anatase in the course of heating before and after anatase-to-rutile phase transformation. When niobium ions enter substitutionally into TiO_2, the charge of the niobium(V) is kept by the compensation for introductions of structural defects and an appearance of titanium(III) in the niobium-doped TiO_2, $Ti_{1-X}Nb_XO_2$ as shown in the result of EPR measurement (Fig. 6). On the other hand, the charge balance is kept without structural defects and an appearance of titanium(III) by the entrance of M(III) ions substitutionally into TiO_2 as compensation for the introduction of niobium(V) ions in the case of $M(III)_XTi_{1-2X}Nb_XO_2$ [30, 31]. Hydrothermally prepared metastable niobium-doped anatase having these structural defects and the presence of titanium(III) gradually becomes unstable accompanied with increase in crystallinity and crystallite growth of anatase with increasing heat-treatment temperature. In the region of 500–750 °C, niobium component insoluble into anatase structure is gradually segregated and precipitated as Nb_2O_5 and $TiNb_2O_7$ phases out of anatase structure accompanied with decrease in lattice parameters before the phase transformation.

Anatase-to-rutile phase transformation

It is well known that the polymorphic transformation of ceramic materials depends on their grain size, impurities, composition, processing route, the nature and the amount of dopant, and so on. It has been summarized that the addition of Li^+, Cu^{2+}, Co^{2+}, Fe^{3+}, and Mn^{4+} as oxides or fluorides into TiO_2 assists the anatase-to-rutile phase transformation while Nb_2O_5, PO_4^{3-}, and SO_4^{2-} retard the

conversion. Shannon and Pask [4] and Mackenzie [6] explained the accelerating effect of Cu^{2+}, Co^{2+} etc. by assuming that these ions substitute for Ti^{4+} with the formation of oxygen vacancies. The oxygen vacancies act as nucleation sites for the anatase-to-rutile phase transformation. On the contrary, the inhibiting effect of phosphate and sulfate is explained by Shannon and Pask [5] by assuming that the substitution of S^{6+} and P^{5+} would tend to reduce the number of oxygen vacancies in a way similar to that reported in the case of doping with Nb_2O_5 [6]. Criado and Real [33] concluded that the anatase-to-rutile polymorphic transformation is started by nucleation on the surface of the oxide when the sample undergoes either thermal or mechanical treatment. When niobium is doped substitutionally into TiO_2, the charge of Nb(V) is compensated for a formation of Ti(III) and a decrease in oxygen vacancies in relation to the inhibition of the phase transformation, which receives a support from the detection of Ti(III) via EPR measurements, the change in color of sample powders, and absorption in the visible region in this study.

Figure 10 shows XRD patterns of the samples containing 8.3 mol.% niobium after heating at 800–980 °C for 1 h. With increasing heating temperature from 920 to 980 °C, the intensity of the diffraction peaks of rutile-type titania increased, and the intensity of the anatase-type titania decreased, although the change in the intensity of the diffraction peaks of $TiNb_2O_7$ phase hardly observed.

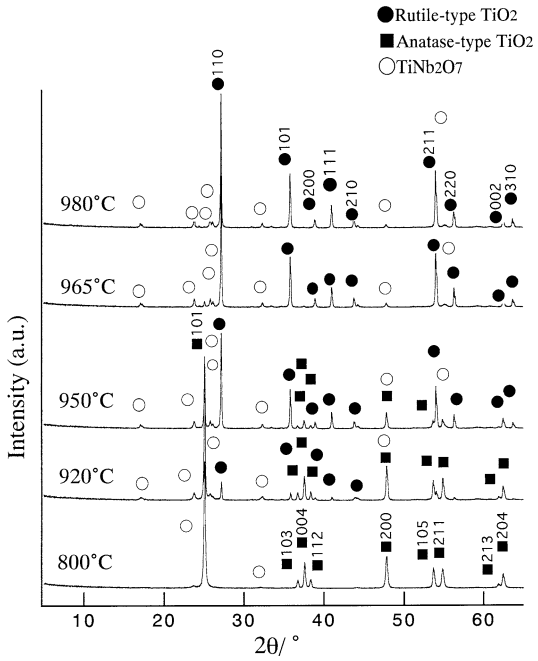

Fig. 10 X-ray diffraction patterns of 8.3 mol.% niobium containing titania heated at 800–980 °C for 1 h in air

Figure 11a shows XRD patterns of the samples containing 35.8 mol.% niobium after heating at 950–1,100 °C for 1 h. Figure 11b shows the detail of the region around $2\theta = 22$–$28°$ in the XRD patterns of the samples. The anatase-type titania and $TiNb_2O_7$ phase were only detected as crystalline phase in the samples after heated at 950–1,000 °C for 1 h, and no trace of diffraction peaks due to rutile phase were detected. The anatase phase was fully maintained after heated at 1,000 °C for 1 h by the presence of niobium component. The partial phase transformation from anatase to rutile phase was detected in the sample heated at 1,050 °C for 1 h. The phase transformation was already concluded in the sample heated at 1,150 °C.

The anatase-to-rutile phase transformation ratio for the present samples is plotted as a function of heating temperature in Fig. 12. The phase transformation started at 850 °C and ended at >950 °C for the pure TiO_2 hydrothermally prepared. The starting and ending temperature of the phase transformation were gradually shifted to higher temperature with increased niobium content in the samples. The starting and ending temperature were delayed from 850 to >1,000 °C and from 950 to >1,100 °C, respectively, when the sample contained 35.8 mol.% niobium. Most of the niobium component hydrothermally doped into metastable anatase structure were separated by crystallization as Nb_2O_5 and $TiNb_2O_7$ phases out of the anatase before the phase transformation in the course of heating. Thus, it is presumed that there is little difference in the amount of niobium remained in the anatase among the samples after heated at or more than 800 °C. However, the phase transformation temperature was gradually delayed with increasing niobium content hydrothermally doped into the anatase samples. It is suggested that the precipitation process of $TiNb_2O_7$ out of the anatase phase and the microstructure of the composite powders consisting with anatase and $TiNb_2O_7$ phase affect the diffusion of TiO_2, and suppress both the crystallite growth of anatase and the resultant nucleation of rutile phase.

Conclusion

Nanoparticles of anatase-type titania containing niobium were hydrothermally precipitated at 240 °C for 5 h from the amorphous co-precipitates that were formed from the precursor solutions of $TiOSO_4$ and $NbCl_5$. The anatase phase was fully maintained after heating at 850–1,000 °C for 1 h by the presence of niobium component, but most of the added niobium component that was separated from the anatase phase at >800 °C was precipitated as Nb_2O_5 and $TiNb_2O_7$ phases out of the anatase, which is accompanied with decrease in the lattice parameters a_0 and c_0 of anatase. The phase transformation from anatase to rutile structure

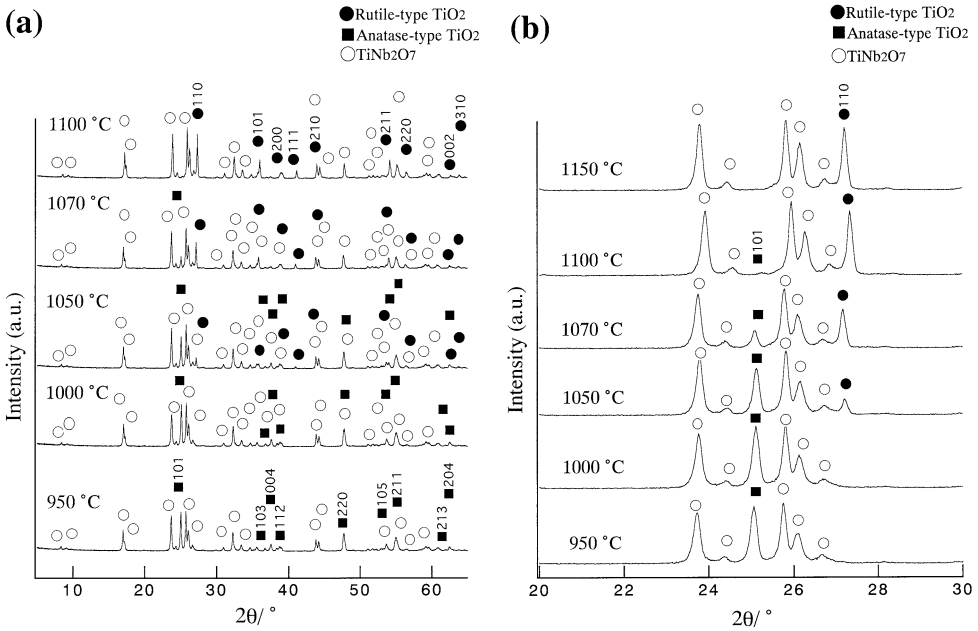

Fig. 11 **a** X-ray diffraction patterns of 35.8 mol.% niobium containing titania heated at 950–1,100 °C for 1 h in air. **b** Detail of the region around 25° 2θ of the X-ray diffraction patterns of 35.8 mol.% niobium containing titania after heated at 950–1,150 °C for 1 h in air

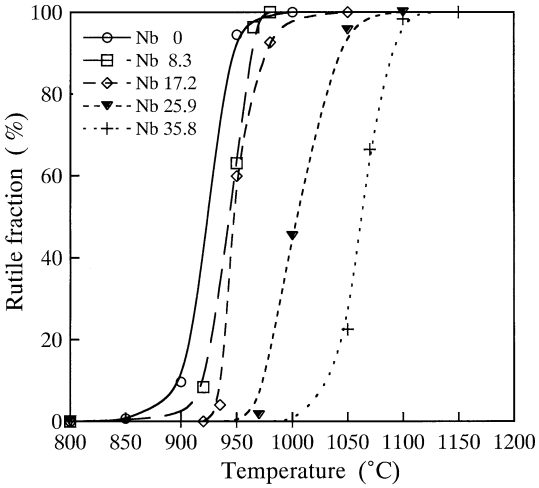

Fig. 12 Phase transformation from anatase-type to rutile-type structure for titania containing 0–35.8 mol.% niobium plotted against heating temperature

was delayed by the presence of niobium component. The as-prepared niobium-doped anatase-type titania showed bluish color and absorption in the visible region, which was confirmed to be due to the presence of Ti(III) in the solid solutions using EPR measurements. The confirmation of no signal corresponding to Nb^{4+} suggested that the doped niobium in the samples existed as valence of five.

Acknowledgements The authors thank Shingo Sato for his assistance. The present work was partly supported by Grant-in Aids No. 21560703 for Scientific Research from the Ministry of Education, Culture, Sports, Science, and Technology of Japan.

References

1. Fox MA, Dulay MT (1993) Chem Rev 93:341
2. O'Regon B, Gratzel M (1991) Nature 353:737
3. Ferroni M, Guidi V, Martinelli G, Faglia G, Nelli P, Sberveglieri G (1996) Nanostruct Mater 7:709
4. Shannon RD, Pask JA (1965) J Am Ceram Soc 48:391
5. Shannon RD, Pask JA (1964) Am Miner 49:1707
6. Mackenzie KJD (1975) Trans J Br Ceram Soc 74:77
7. Suyama Y, Kato A (1978) J Ceram Soc Jpn 86:119 [in Japanese]
8. Hishida S, Tanaka M, Yanagida H (1978) J Ceram Soc Jpn 86:631
9. Leduc CA, Campbell JM, Rossin JA (1996) Ind Eng Chem Res 25:2473
10. Gennari FC, Pasquevich DM (1998) J Mater Sci 33:1571. doi: 10.1023/A:1017515804370
11. Hirano M, Joji T, Inagaki M, Iwata H (2004) J Am Ceram Soc 87:35
12. Hirano M, Ota K, Ito T (2005) J Am Ceram Soc 88:3303
13. Oliveri G, Ramis G, Busca G, Escribano VS (1993) J Mater Chem 3:1239
14. Rao CNR, Turner A, Honig JM (1959) J Phys Chem 11:173
15. Ding XZ, Liu XH (1998) J Mater Res 13:2556
16. Deo G, Turek AM, Wachs IE, Machej T, Haber J, Das N, Eckert H, Hirt AM (1992) Appl Catal A 91:27
17. Dutta PK, Ginwalla A, Hogg B, Patton BR, Chwieroth B, Liang Z, Gouma P, Mills M, Akbar S (1999) J Phys Chem B 103:4412
18. Hirano M, Ota K, Iwata H (2004) Chem Mater 16:3725
19. Czanderna AW, Rao CNR, Honig JM (1958) Trans Faraday Soc 54:1069
20. Yoganarasimhan SR, Rao CNR (1962) Trans Faraday Soc 58: 1579
21. Hirano M, Morikawa H (2003) Chem Mater 15:2561
22. Hirano M, Matsushima K (2006) J Am Ceram Soc 89:110
23. Hirano M, Nakahara C, Ota K, Tanaike O, Inagaki M (2003) J Solid State Chem 170:39
24. Hirano M, Date K (2005) J Am Ceram Soc 88:2604
25. Tanabe K, Okazaki S (1995) Appl Catal A Gen 133:191

26. Zhang Z, Wang CC, Zakaria R, Ying JY (1998) Phys Chem B 102:10871
27. Zakrzewska K, Radecka M, Rekas M (1997) Thin Solid Films 310:161
28. Sharma RK, Bhatnagar MC (1999) Sens Actuators B 56:215
29. Hirano M, Matsushima K (2006) J Nanosci Nanotechnol 6:762
30. Hirano M, Ito T (2006) J Nanosci Nanotecnol 6:3820
31. Hirano M, Ito T (2008) Mater Res Bull 43:2196
32. Spurr RA, Myers H (1957) Anal Chem 29:760
33. Criado BJ, Real C (1983) J Chem Soc Faraday Trans 1 79:2765